ISSN 0020-4412, Instruments and Experimental Techniques, 2021, Vol. 64, No. 1, pp. 63–70. © Pleiades Publishing, Ltd., 2021.
Russian Text © The Author(s), 2021, published in Pribory i Tekhnika Eksperimenta, 2021, No. 1, pp. 72–80.

NUCLEAR EXPERIMENTAL TECHNIQUE

Nondestructive Elemental Diagnostics of the Fuel-Rod Cladding Surface by the Ion-Beam and X-Ray Analytical Methods

V. K. Egorov[a,*], E. V. Egorov[a,b,c], B. A. Kalin[d], and D. A. Safonov[d]

[a] *Institute of Microelectronics Technology and High-Purity Materials, Russian Academy of Sciences, Chernogolovka, Moscow oblast, 142432 Russia*

[b] *Kotel'nikov Institute of Radioengineering and Electronics (IRE), Russian Academy of Sciences, Moscow, 125009 Russia*

[c] *Financial University under the Government of the Russian Federation, Moscow, 125993 Russia*

[d] *National Research Nuclear University, Moscow Engineering Physics Institute, Moscow, 115409 Russia*

**e-mail: egorov@iptm.ru*

Received July 19, 2020; revised August 9, 2020; accepted August 10, 2020

Abstract—The characteristics of the production technology for fuel rod cladding oriented to its application for water-moderated water-cooled power reactors with a coolant temperature of 300–350°C are presented. Possible directions for the modification of the cladding surface are proposed. The methodological background for the diagnostics of materials based on the ion-beam and X-ray diagnostic methods is discussed. Using this diagnostics, it is possible to characterize the parameters of the inner and outer surfaces of the fuel-rod cladding without changing its form. Experimental data are presented, which demonstrate the efficiency of the proposed analytical complex for characterizing the surface layers of fuel-rod cladding.

DOI: 10.1134/S0020441221010085

INTRODUCTION

Nuclear reactors that operate using thermal-neutron fluxes, i.e., the so-called water-moderated water-cooled power plants, form the basis of modern nuclear power engineering. Plants of this type that operate at temperatures of 300–350°C in the reactor core are the most widespread. Under these conditions, a superheated water–vapor mixture, on the one hand, is a carrier of thermal energy from fuel rods located in a nuclear reactor to the second water circuit that serves the steam generator and, on the other hand, is a medium for moderating the neutron flux. Fuel rods in these plants play the role of converters of the energy released by nuclear reactions into heat. Heat is generated by nuclear fragments that occur during the decay of uranium nuclei under exposure to a thermal-neutron flux and lose their energy in the material of the fuel pills. This energy is removed through the cladding of the fuel rod by the coolant that passes over it. In principle, the design of the fuel rod is quite simple. It consists of a thin-walled cylindrical cladding that holds nuclear fuel. Uranium oxide prepared in the form of a pill with a central hole is the nuclear fuel material for such fuel rod. The longitudinal cross section of a fuel rod with such a design is shown in Fig. 1. Although the design of the fuel rod is apparently simple, its production technology is a complex multifunctional procedure with a set of specific requirements for the selection of the cladding material and a sequence of technological operations that guarantee its mechanical, corrosion, and radiation resistance during long-term operation as a nuclear-reactor component.

The lowest level of neutron absorption is the most important requirement for the selection of a material for fuel-rod cladding. Experimental investigations have shown that magnesium, aluminum, and zirconium nuclei are characterized by a small neutron-cap-

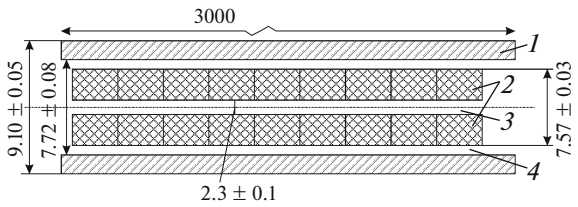

Fig. 1. The longitudinal cross section of a fuel rod of a water-moderated water-cooled power reactor: (*1*) metal cladding of the fuel rod, (*2*) nuclear fuel pill, (*3*) technological hole in the pills, and (*4*) clearance between the fuel pills and the cladding, which is filled with ^{4}He under pressure.

ture cross section [1]. The thermal conductivity and mechanical stability of a fuel-rod structure are factors of the same importance. The degree of corrosion resistance of the cladding of a fuel element is determined by the properties of its outer and inner surfaces. Since an entire set of requirements is imposed on the fuel-rod cladding material, the specific choice turns out to be a compromise. Experimental experience has shown that zirconium doped with a small amount of niobium is the most suitable material for manufacturing the fuel-rod cladding for water-moderated water-cooled nuclear reactors with operating temperatures of 300–350°C in their cores [2].

The technology for manufacturing thin-walled tubular claddings from this material is rather laborious [3]. First, the starting Zr must be purified of impurities, especially of hafnium. Second, the procedure for obtaining long thin-walled pipes should provide constancy of the wall thickness along the entire pipe length, as well as the homogeneity of the structure and composition of the material. Further, while carrying out measures for increasing corrosion resistance, the modification procedure must provide the constancy of the properties along the entire length of the cladding. At the present stage of the development of water-moderated water-cooled nuclear reactor technology, the problem of long-term corrosion resistance of fuel-rod claddings has become a significant obstacle to increasing their efficiency. Therefore, attempts were made to perform implantation [4] and diffusion [5] modifications of the surface of fuel-rod claddings and to use various anticorrosive coatings [6].

At the same time, both the technology for modifying the surfaces of the fuel-rod cladding and the studies of the surface layers of claddings on fuel elements that have completed a full radiation cycle require a complex of nondestructive elemental and structural diagnostics of the surface without changing the shape of cladding elements. In this paper, we propose a methodological base for a complex of analytical diagnostics that uses the ion-beam and X-ray methods for studying materials.

ION-BEAM AND X-RAY POTENTIALS FOR THE DIAGNOSTICS OF FUEL-ROD SURFACES

Analytical diagnostics of film coatings of material objects with their surface layers modified using various methods can be performed by a number of diagnostic techniques [7–12]. Their selection is determined, on the one hand, by the possibilities of elemental and structural analysis, and, on the other hand, by the expected thickness of coatings or the depth of surface modification. The task of increasing the corrosion resistance of fuel-rod claddings involves both modification of their outer and inner surfaces to a depth ranging from a few nanometers to several micrometers, and development of technologies for obtaining protective coatings with a thickness of several micrometers. In this case, it is supposed that elemental and structural diagnostics of modified regions will be performed without changing the shape of tubular claddings. High-efficiency elemental–dimensional analysis of films and surface layers of materials with nanoscale thicknesses may be performed using the method of Rutherford backscattering (RBS) of high-energy beams of helium and hydrogen ions on test samples [13]. This method is applicable in ion-beam analytical systems, e.g., in the Sokol-3 complex [14]. This method is aimed at determining the elemental concentration profile for the distribution of elements over the thickness of the surface layer of a material to a depth of 2 μm with a resolution of approximately 10 nm when using $^4He^+$ ion beams and to a depth of up to 15 μm with a resolution of approximately 30 nm when using scattering of hydrogen ion beams. The characteristic X-ray fluorescence yield is measured in parallel with making RBS measurements to diagnose the presence of trace impurities in materials. The detection limits of these measurements are at a level of 10^{-6} at % and are better if special geometry is used [15]. The schematic diagram of the experimental chamber in the Sokol-3 ion-beam analytical complex with a system for detecting scattered ions and measuring the X-ray fluorescence yield is shown in Fig. 2. The RBS method is a nondestructive method owing to the low values of analytical radiation doses and it is the only absolute instrumental method for elemental diagnostics of materials. The absoluteness of measurements is achieved by normalizing the measured scattering spectra to the total number of ions that hit the test sample during a measurement session. All measurements are carried out under medium vacuum conditions of 10^{-3}–10^{-4} Pa. The experimental spectra obtained at the Sokol-3 complex are fitted using the RUMPP computer program, which is an upgraded version of the RUMP program [16].

Figure 3 shows the layouts for performing ion-beam and ion–X-ray fluorescence diagnostics of the inner and outer surfaces of tubular-structure elements without their deformation. Since the diameter of the ion probe is 1 mm, the proposed geometry of measurements will not distort the results of ion-beam and X-ray elemental diagnostics of the inner and outer surface layers of fuel-rod claddings in their initial state, after their modification, and after actual functioning of a fuel rod in a nuclear reactor.

As an additional X-ray diagnostic approach to studying changes in the elemental composition over the thickness of the surface layers on the inside and outside of fuel rods, we used an original concept of the method that we developed for carrying out X-ray fluorescence analysis under conditions of total external reflection of the exciting hard X-ray flux from the surface under study (TXRF) [17]. The most important feature of standard TXRF measurements is the use of

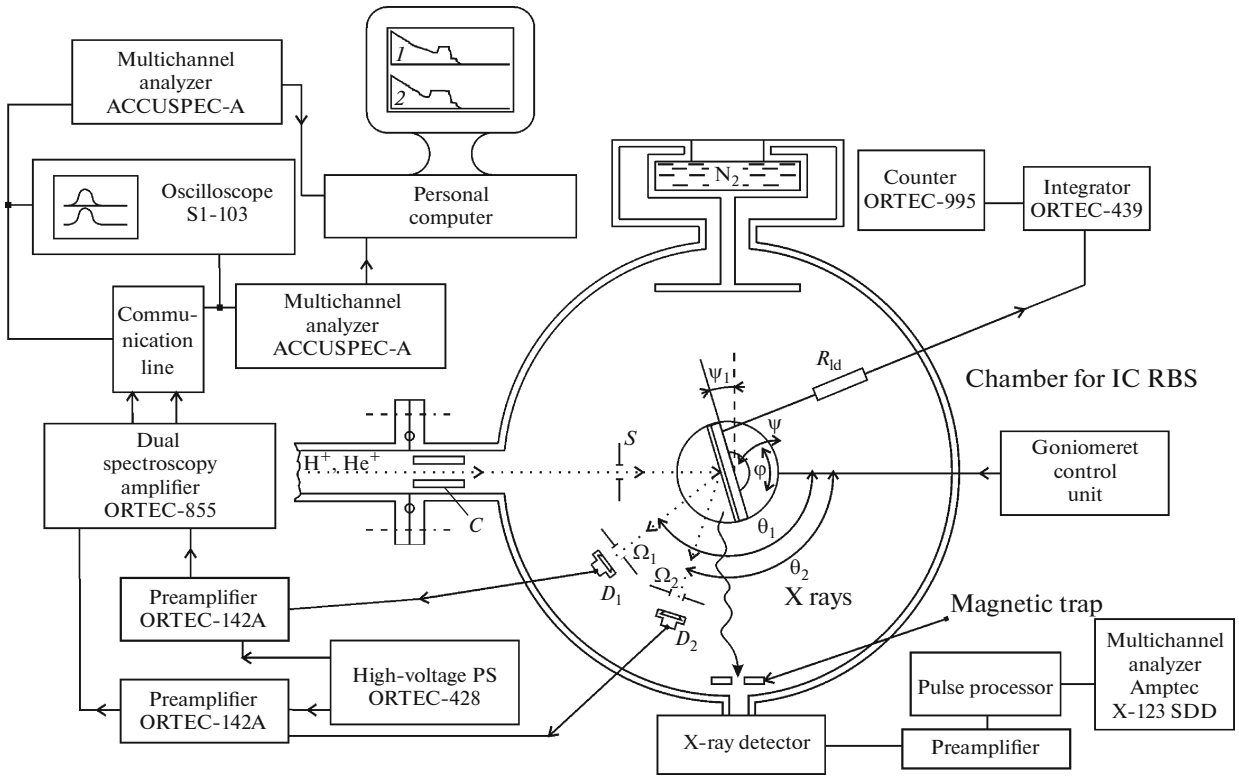

Fig. 2. The diagram of the vacuum chamber for RBS and X-ray fluorescence analysis of test samples using the Sokol-3 analytical complex and the system for detecting scattered ions and measuring the X-ray fluorescence yield: (PS) power supply, (*S*) protective shield, (R_{ld}) load resistance (~1 kΩ), (*C*) ion collimator, (D_1, D_2) scattered-ion detectors, (Ω_1, Ω_2) solid angles of scattered-ion detection, (θ_1, θ_2) angles of scattered-ion detection, (ψ, φ) angles of spatial orientation of the target, (ψ_1) angle of inclination of the target to prevent channeling, and (IC) ion channeling.

the phenomenon of total external reflection of an exciting flux, within which characteristic X-ray fluorescence is generated by the near-surface layer of a test sample with a thickness of 3–5 nm. As a result, this method is characterized by a sharp decrease in the detection limits for impurities in comparison with the X-ray fluorescence analysis in a standard geometry and with the electron microprobe analysis. In addition, data from research carried out using TXRF spectrometry are free from the influence of the matrix effect. The idea behind the modified TXRF approach is illustrated by the layout of measurements presented in Fig. 4. The diagram shows the radiation source (the focus of an BSV-28 (Ag) X-ray tube); the flux former, which is an assembly of two vertical mutually aligned cutting slits S_1 and S_2 6 μm wide and 10 mm high, which are spaced 100 mm apart [18]; a scintillation detector *D* with its own slit system; a sample holder that is equipped with a horizontal microfeed system; and a semiconductor detector of the characteristic X-ray fluorescence yield. The exciting flux only touches the top of the outer surface of the diagnosed tube sample in Fig. 4a, and Fig. 4b illustrates the situation when the sample completely covers the exciting X-ray microbeam. Since its width in this position of the sample is 15 μm, the semiconductor detector measures the X-ray excitation yield from a 15-μm-thick surface layer of the sample. The developed method for X-ray elemental diagnostics is original; it allows us to analyze the elemental composition to a greater depth in comparison with the ion-beam diagnostics of materials. At the same time, this method cannot provide direct information on the distribution of elements over

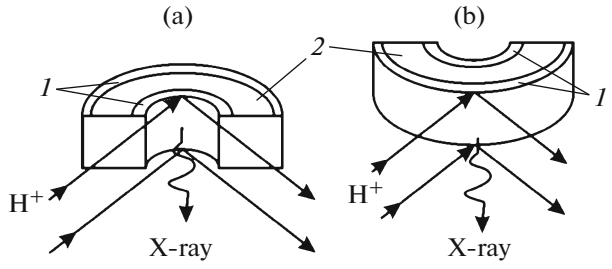

Fig. 3. The layouts of the RBS investigations of the element distribution in the depth of surface layers of (a) the outer and (b) inner surfaces of cylindrical fuel-rod cladding fragments: (*1*) surface layers, (*2*) volume of the cylindrical cladding, and (H^+) primary high-energy proton beam.

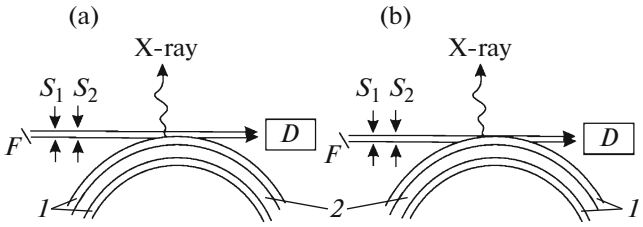

Fig. 4. The diagrams for the diagnostics of the outer surface of a cylindrical fuel-rod cladding using the modified TXRF method (a) under conditions of conventional TXRF geometry and (b) under conditions of complete overlapping of the exciting flux by a fragment of the tested cladding: (*F*) the focus of the BSV-28 (Ag) X-ray radiation source, (*1*) the inner and outer surface layers of the fuel-rod cladding, (*2*) the volume of the fuel-rod cladding, and (*D*) scintillation detector.

depth, since it is not free from the influence of matrix effects and the absorption of excited characteristic radiation in the test sample must be taken into account when interpreting data obtained using it. In addition, certain expansion of the diagnostic area must also be taken into account.

Similar information on the elemental composition of the inner surface layer of a tubular sample can be obtained in the same measurement geometry, but upon a significant (down to 1 mm) decrease in the vertical size of the excitation beam.

The intensity of the transmitted flux measured by the scintillation detector has been selected as a parameter that fixes the thickness of the layer excited by an external X-ray beam.

DIAGNOSTICS OF THE EXTERNAL SURFACE OF THE MODIFIED FUEL-ROD CLADDING

The use of E-110 zirconium alloy with 1 at % niobium as a cladding material for fuel rods has shown its high mechanical and radiation stability under operating conditions in cores of water-moderated water-cooled power plants. At the same time, the experience from long-term operation of reactor units made of this material has demonstrated its insufficient corrosion resistance, especially to the action of a high-temperature steam–water mixture. Therefore, the increase in the operational properties of fuel rods turned out to be directly dependent on improvement in the corrosion properties of the external surface of their claddings. The use of external chromium coatings appeared to be among the most effective means for increasing the corrosion resistance of zirconium–niobium claddings [19]. Therefore, the chromium coating was deposited on the outer surface of the fuel-rod cladding while developing the technology for modifying this cladding. This coating was investigated by making RBS measurements in parallel with probing the outer surface of the cladding without the chromium coating. The experimental and theoretical spectra obtained during these measurements are shown in Fig. 5. The figure also shows the RBS spectrum of a thick zirconium oxide film, which also has prospects of being used as a possible protector against the corrosion action of a high-temperature steam–water mixture. The theoretical approximation of the RBS spectra of compounds that contain zirconium atoms is difficult, since this element, in contrast to the elements located nearby in the periodic table (Y and Nb), is characterized by the presence of a number of stable isotopes (^{90}Zr, 52%; ^{91}Zr, 11%; ^{92}Zr, 17%; ^{94}Zr, 17%; and ^{96}Zr, 3%). The RBS spectrum of H^+ ions (E_0 = 1.186 MeV) from the outer surface of the unmodified cladding sample (Fig. 5a) is a flat spectrogram with a shape ascend in the region of channel 545. The spectrum has a barely noticeable step in the region of channel 436. The fitting processing of the spectrum showed that this step indicates the presence of oxygen atoms in the surface layer several hundred nanometers thick at a level of 2–3 at %. Since the initial composition of the cladding was represented as $Zr_{0.986}Nb_{0.01}Fe_{0.004}$, zirconium oxide may have appeared in the external surface layer of the unmodified cladding in the presence of a low oxygen concentration in the volume.

The experimental and theoretical spectra of H^+ ions (E_0 = 1.187 MeV) in Fig. 5b were obtained for a zirconium oxide (ZrO_2) film. The fitting of the experimental spectrum showed that the thickness of the oxide layer exceeded 10 μm and the composition was close to stoichiometric. These spectra are presented together with the spectra of the original fuel-rod cladding in order to exclude any doubt about the presence of a significant oxygen concentration in its surface layer. The experimental and theoretical RBS spectra of H^+ ions (E_0 = 1.182 MeV) from the outer fuel-rod cladding modified by deposition of the chromium coating on its surface is shown in Fig. 5c. The preliminary fitting of the experimental spectrum showed that a 5.7-μm-thick film containing a significant amount of chromium atoms was result of the deposition procedure on the outer surface of the cladding. This film is characterized by a content of approximately 10 at % of oxygen and the presence of up to 10 at % of either hydrogen or structural vacancies in its structure. Diagnostics of hydrogen in the material was not carried out due to technical difficulties. The channel numbers that correspond to the energies of scattering of hydrogen ions from atomic nuclei located on the surfaces of the test samples are marked in the spectra with arrows.

In parallel with measuring the RBS spectra, we recorded the spectra of the characteristic X-ray measuring from the test samples that were excited by a proton beam incident on these samples. The obtained spectra are shown in Fig. 6. The spectra are presented on a logarithmic scale, since the intensity of the characteristic X-ray fluorescence lines of zirconium and chromium significantly exceeds the intensity of the

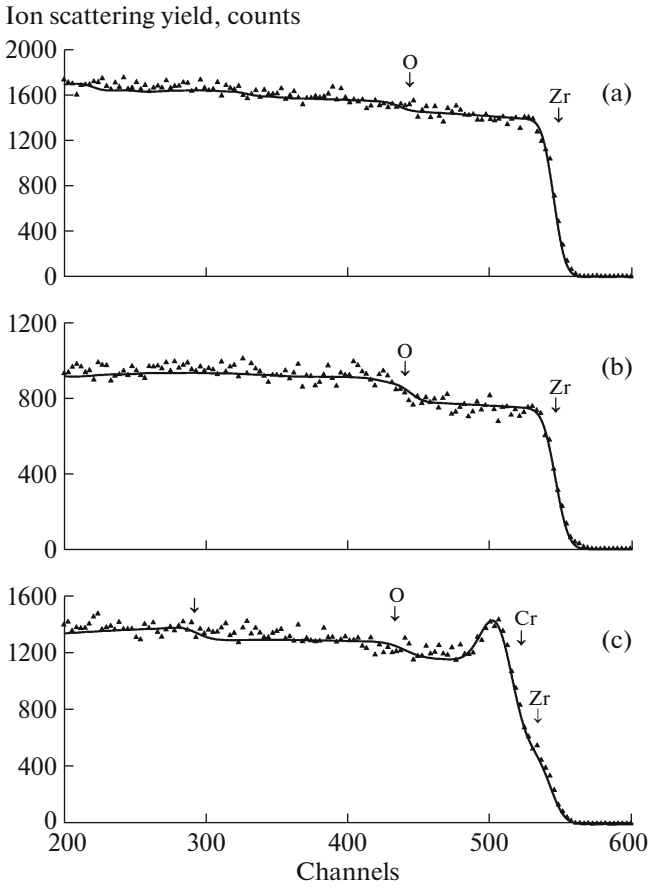

Fig. 5. The RBS spectra of H^+ ions (E = 1.18 MeV) obtained for the external surface of the fuel-rod cladding (a) with the initial structure, (b) with the zirconium oxide film on it, and (c) with the structure modified by deposition of the chromium coating. The arrows indicate the energy of hydrogen-ion scattering from nuclei of surface atoms and the energy characterizing the sharp decrease in the Cr concentration in the target under study. The energy step is 1.9 keV/channel.

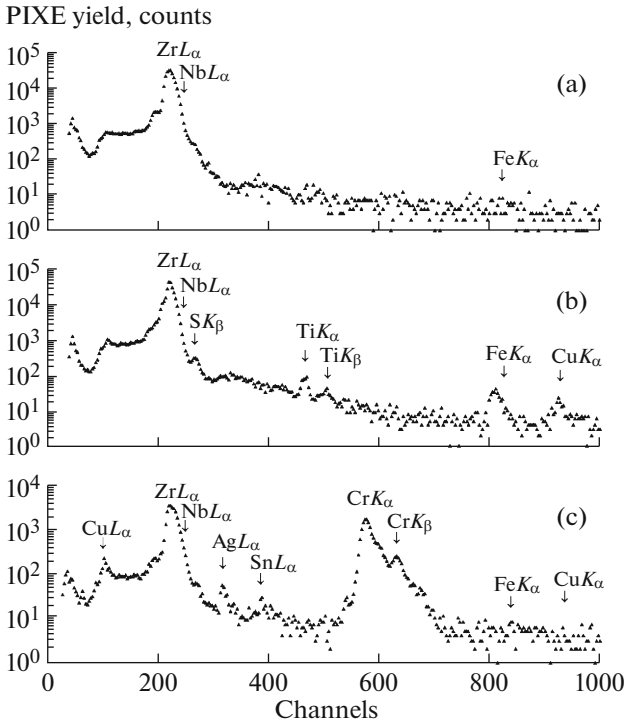

Fig. 6. The PIXE spectra obtained for external surface of the fuel-rod cladding with (a) the initial structure, (b) a thick zirconium oxide film on the outer surface, and (c) the structure modified by the chromium coating deposition. The energy step is 10 eV/channel.

lines of impurity and alloying elements. The spectrum of proton-induced X-ray emission (PIXE) obtained for the outer surface of the unmodified fuel rod cladding (Fig. 6a) demonstrates the observed absence of lines of impurity components, whose content, at least, does not exceed 1 ppm [20]. At the same time, in accordance with the initial data, the cladding material contains niobium atoms at a level of approximately 1 at % and iron atoms with a content of less than 0.04 at % in addition to zirconium atoms. Diagnostics of the presence or absence of oxygen atoms in the test sample is impossible for technological reasons. The point is that the X-ray detector built into the experimental chamber of the Sokol-3 complex is equipped with an 8-μm-thick entrance Be window, which completely absorbs the emission of the characteristic oxygen line $O K_\alpha$ (E = 0.523 keV). The $Nb L_\alpha$ line, whose position corresponds to channel 220, is completely masked by a high-intensity $Zr L_{\alpha\beta\gamma}$ peak. The presence of Fe atoms in the cladding material is found by a barely noticeable irregularity in the spectrum region of channel 830. It should be borne in mind that ion-beam diagnostics has a local character, as the diameter of the ion probe is 1 mm. The low intensity of the $Fe K_\alpha$ line in the presented spectrum indicates that the distribution of iron atoms in the material of the fuel-rod cladding was inhomogeneous. The content of Fe atoms was quantitatively estimated on the basis of averaged results of measurements at a number of successive points.

The PIXE spectrum in Fig. 6b, which was obtained for the zirconium oxide sample, demonstrates a greater elemental diversity. The material contains S atoms at a level of a few ppm, as well as Cu and Ti atoms at a level of several hundred ppm. The $Nb L_\alpha$ line also turns out to be masked by the intense $Zr L_{\alpha\beta\gamma}$ peak. The spectrum contains lines of unidentified elements. As was the case with the previous spectrum, the $Zr K_\alpha$ (E = 15.77 keV) and $Zr K_\beta$ (E = 17.67 keV) lines are absent in the diagram, since the measurable energy range is limited to 10 keV.

The PIXE spectrum in Fig. 6c, which was obtained for the external surface of the fuel-rod cladding modified by deposition of the chromium coating, demonstrates two intense lines: $Zr L_{\alpha\beta\gamma}$ and $Cr K_{\alpha\beta}$. In addition

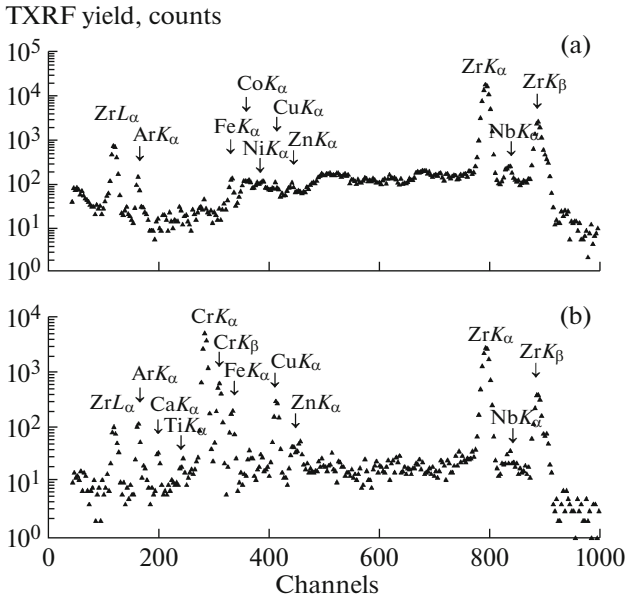

Fig. 7. The TXRF spectra obtained for external surface of the fuel-rod cladding with (a) the initial structure and (b) the structure modified by the chromium-coating deposition. The energy step is 20 eV/channel.

to these lines, the spectrum contains the FeK_α, SrL_α, AgL_α, and CuL_α lines. It should be noted that low-energy X-ray fluorescence lines are excited well under the conditions of PIXE measurements in comparison with lines that correspond to higher energies. Therefore, the TXRF spectra obtained for the external surface of the original and modified fuel-rod cladding are shown in Fig. 7 in addition to the PIXE studies. These spectra were recorded in the geometry of total external reflection at a zero angle of incidence of the AgK_α excitation beam under conditions of beam contact with the outer surface of the test sample (Fig. 4a). A significant difference between the data obtained in the TXRF measurements from the PIXE elemental diagnostics reflects the fact that these data are averaged over the entire excited surface layer of this sample.

The X-ray fluorescence spectrum shown in Fig. 7a, which characterizes the elemental composition of the outer surface layer of the unmodified fuel-rod cladding, shows that zirconium is the main element of this layer, which is ~5 nm thick. Since the matrix effect and the effect of characteristic X-ray fluorescence absorption in the sample material are absent and the cross sections for fluorescence excitation zirconium and niobium atoms by the AgK_α flux are equal, the relative concentration of these elements in the excited layer can be calculated based on the ratio of the integral intensities for their X-ray fluorescence lines. This relationship shows that the concentration of Nb atoms in the surface layer is 1.25 at %. The spectrum also contains the Zr$L_{\alpha\beta\gamma}$ line, but its intensity is immeasurably lower than its intensity in the spectrum obtained in the PIXE measurements; in addition, the acquisition time for PIXE spectra is shorter by an order of magnitude than the acquisition time of TXRF spectra. Moreover, the spectrum contains an ArK_α line (E = 2.957 keV), which reflects the fact that the measurements are made in air, and a number of lines that characterize the presence of impurities in the cladding material (FeK_α, CoK_α, NiK_α, CuK_α, and ZnK_α). The content of Fe atoms is close to 0.08 at %, and the concentration of other impurities does not exceed 0.05 at %.

The TXRF spectrum obtained for the surface of the modified fuel-rod cladding (Fig. 7b) demonstrates significant changes compared to the spectrum that characterizes the unmodified surface. The spectrum contains two intense doublets, CrK_α–K_β and ZrK_α–K_β, the Zr$L_{\alpha\beta\gamma}$ and ArK_α lines, as well as a number of alloying (FeK_α and CuK_α) and impurity (CaK_α, TiK_α, ZnK_α, and GaK_α) elements. All of this set of elements characterizes the thin surface layer of the cladding, which was modified by deposition of the chromium coating. Its estimated thickness, was 5 mm. The presented TXRF spectrum suggests that during the deposition of the chromium coating, the deposited chromium atoms were mixed with the structure-forming substrate material, seemingly, with the formation of the intermetallic compound $ZrCr_2$. In this case, the concentration of alloying components in the thin surface layer was 8–10 at % of each element. Moreover, the presence of a few oxygen and hydrogen atoms in the film coating can be expected, which seemed very likely when the RBS spectrum of this sample was fitted.

Further investigations of the outer surface of the fuel-rod cladding modified by deposition of the chromium coating on it were carried out using X-ray radiation. The method of originally modified spectrometry is reassembling on the investigations under conditions of total external reflection of the excitation beam. Figure 8 shows the geometry of measurements and presents the experimental data obtained upon changing the position of the test sample of the modified fuel-rod cladding relative to the exciting X-ray beam along the direction of the X axis. The obtained experimental diagram shows the dependences of the integral X-ray fluorescence intensities of the lines of elements contained in the diagnosed layer on the depth of penetration of the exciting radiation flux into the material of the modified cladding from its outer side. As the excitation flux deepens into the cladding material, a sharp increase in the X-ray fluorescence intensity of chromium and zirconium is observed. At the same time, no increase in the X-ray fluorescence intensity for the FeK_α and CuK_α lines is observed. This indicates that copper and iron atoms are mainly concentrated in a thin near-surface layer of the obtained coating with a thickness of up to 10 nm, which largely consists of the intermetallic compound $ZrCr_2$. As the beam deepens, the ratio between the output intensities

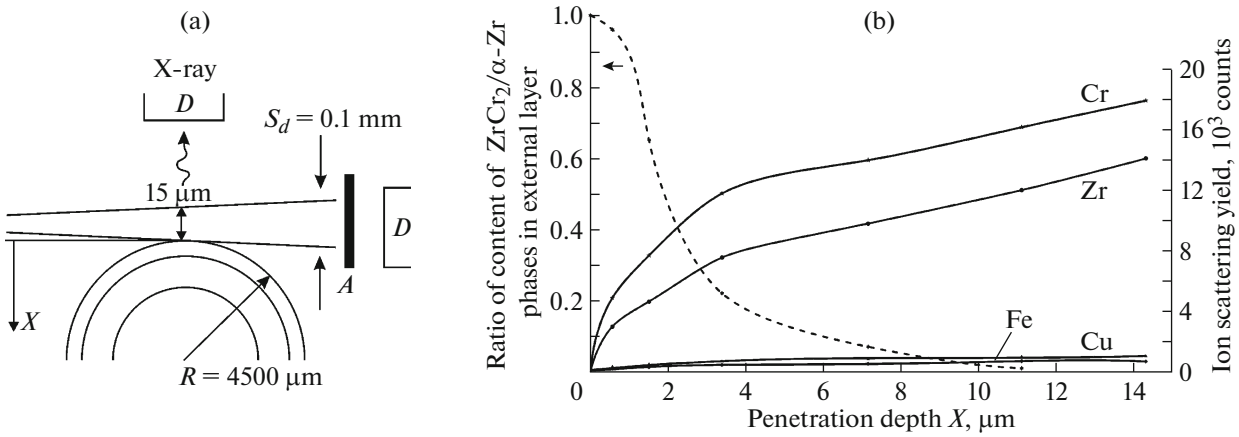

Fig. 8. (a) The diagram of measurements of the X-ray characteristic fluorescence yield, which is a specific modification of TXRF measurements, and (b) the diagrams for the ZrK_α, CrK_α, CuK_α, and FeK_α fluorescence yields for the external surface of the fuel-rod cladding modified by deposition of a chromium coating, vs. the penetration depth of the exciting beam (AgK_α) into the cladding and vs. the ratio of the content of the $ZrCr_2$/α-Zr phases in it: vs. the depth (*A*) flow damper.

of the ZrK_α and CrK_α lines begins to change from 1 : 2 to 1 : 1. This suggests that the protective chromium coating is a mixture of the intermetallic compound and α-zirconium with a gradual increase in the proportion of α-zirconium with a decrease in the distance to the coating/substrate interface. At the same time, it should be recognized that these results are purely qualitative, since it is clear from geometric considerations that when the fuel-rod cladding is deepened into the exciting flow, the change in the X-ray fluorescence intensity is no longer a direct reflection of the distribution of atoms over the coating thickness.

DISCUSSION

The methodological approach proposed in this paper was used to study the elemental composition of the outer surface of fuel-rod claddings before and after modification by deposition of a chromium film coating and demonstrated its fundamental efficiency. The comparative studies of the modified and unmodified outer surface of the fuel-rod cladding using the RBS method allowed us to ascertain that the thickness of the chromium coating was 5.7 μm and that it could contain some oxygen and, presumably, hydrogen. Niobium with a content of 1.25 at % was used as the main alloying element in the bulk of the cladding material, and Fe with a content of about 0.08 at % was used as an additional alloying element. The modified TXRF method for studying the elemental composition of materials made it possible to determine that the chromium coating in the 10-nm-thick surface layer was most likely composed of the intermetallic compound $ZrCr_2$, while the alloying elements Cu and Fe were concentrated in this surface layer. The measurements showed that the chromium concentration in the coating decreased with an increase in the depth of testing and dropped to its concentration in the α-Zr solid solution at a depth of about 6 μm. In accordance with the phase diagram of the Cr–Zr system shown in Fig. 9, the Cr content of the α-Zr solid solution did not exceed 0.5 at %. In the continuation of this research, it is necessary to deposit a chromium coating on fuel-rod claddings and perform their heat treatment under various conditions in order to obtain detailed information on the formation of the protective surface layer of coatings. The problem of the oxygen content in the original and modified cladding surfaces can be successfully solved by complementing the instrumentation of the analytical chamber of the Sokol-3 complex with an X-ray detector with an ultrathin entrance window, which allows measuring the X-ray fluorescence yield of the OK_α line.

The problem of the possible presence of hydrogen in the surface cladding layers can be solved by applying recoil nuclear spectrometry [22], which has been successfully used, in particular, in the study of perovskites using the Sokol-3 complex [23]. The proposed methodological complex can be expanded by introducing diffractometric studies of the inner and outer surfaces of claddings into its program to determine the phase relations. In future studies, we are planning to investigate not only claddings intended for model research, but also elements of claddings that have operated in actual nuclear reactors.

CONCLUSIONS

The main objective of the presented work was to develop a concept for effective elemental diagnostics of the fuel-rod cladding surface without changing the shape of this cladding. The preparation of such claddings is a delicate multistage process in which it is not only the elemental composition of a material inside

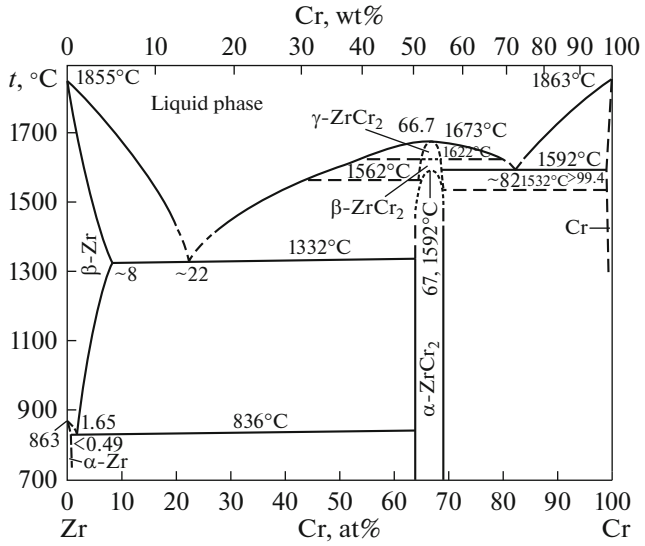

Fig. 9. The Cr–Zr phase diagram [21].

the cladding that plays a significant role, but also the elemental composition of its surfaces. Therefore, a change in the shape when performing analytical activities may affect the diagnostic results. Our work in this direction is pioneering and therefore is not free from drawbacks. The method for modified TXRF material diagnostics is exclusive. Its full methodological basis will be presented in subsequent publications.

FUNDING

The work was carried out in frame of state task 075-00475-19-00 and with the partial financial support of RFBR grants No. 19-07-00271.

REFERENCES

1. Beskorovainyi, N.N., Kalin, B.A., Platonov, P.A., and Chernov, I.I., *Konstruktsionnye materialy yadernykh reaktorov* (Structural Materials for Nuclear Reactors), Moscow: Energoatomizdat, 1995.
2. Zaimovskii, A.S., Nikulina, A.V., and Reshetnikov, F.G., *Tsirkonievye splavy v atomnoi energetike* (Zirconium Alloys for Nuclear Power Engineering), Moscow: Energoatomizdat, 1994.
3. *Razrabotka, proizvodstvo i ekspluatatsiya teplovydelyayushchikh elementov energeticheskikh reaktorov* (Development, Manufacturing, and Operational Process for Heat Emitting Elements of Power Reactors), Reshetnikov, F.G., Ed., Moscow: Energoatomizdat, 1995, book 1.
4. Wu, A., Ribis, J., Brachet, J.C., Clouet, E., Lepretre, F., Bordas, E., and Arnal, B., *J. Nucl. Mater.,* 2018, vol. 504, p. 289. https://doi.org/10.1016/j.jnucmat.2018.01.029
5. Matveev, A.V., Belykh, T.A., Perekhozhev, V.I., Sinel'nikov, L.P., Kruzhalov, A.V., Neshov, F.G., and Trifanov, A.G., RF Patent 2199607, *Byull. Izobret.,* 2003, no. 6.
6. Ivanova, S.V., Glagovskii, E.M., Khazov, I.A., Orlov, V.K., Shlepov, I.A., Nikitin, K.N., Dubrovskii, Yu.V., and Denisov, E.A., *Fiz. Khim. Obrab. Mater.,* 2009, no. 3, p. 5.
7. Woodruff, D.P. and Delchar, T.A., *Modern Techniques of Surface Science (Cambridge Solid State Science Series),* Cambridge: Cambridge Univ. Press, 1986.
8. Potapov, A.I. and Syas'ko, V.A., *Nerazrushayushchie metody i sredstva kontrolya tolshchiny pokrytii i izdelii* (Nondestructive Methods and Means for Testing the Thickness of Coatings and Devices), St. Petersburg: Gumanistka, 2009.
9. Feldman, L.C. and Mayer, J.W., *Fundamentals of Surface and Thin Film Analysis,* Amsterdam: North Holland, Elsevier Science Publ., 1986.
10. Schmidt, B. and Wetzig, K., *Ion Beams in Material Processing and Analysis,* Wein: Springer, 2013.
11. Birkholz, M., *Thin Film Analysis by X-Ray Scattering,* Weinheim: Wiley-VCH, 2006.
12. *X-Ray Spectrometry, Recent Technological Advances,* Tsuji, K., Injuk, J., and Van Grieken, R., Eds., New York: Wiley, 2004.
13. Egorov, V.K., Egorov, E.V., and Afanas'ev, M.S., *J. Surf. Invest.: X-ray, Synchrotron Neutron Tech.,* 2013, vol. 7, no. 4, p. 640.
14. Egorov, V.K. and Egorov, E.V., *NBIKS-Nauka. Tekhnol.,* 2019, vol. 3, no. 7, p. 29.
15. Egorov, V., Egorov, E., and Afanas'ev, M., *J. Phys.: Conf. Ser.,* 2017, vol. 808, no. 1, p. 012002. https://doi.org/10.1088/1742-6596/808/1/012002
16. Doolittle, L.R., *Nucl. Instrum. Methods,* 1985, vol. 9, p. 344.
17. Klockenkamper, R. and von Bohlen, A., *Total X-ray Fluorescence Analysis and Related Methods,* New York: Wiley, 2015.
18. Bykov, V.A., Egorov, V.K., and Egorov, E.V., RF Patent 2486626, *Byull. Izobret.,* 2013, no. 18.
19. Kuprin, A.S., Belous, V.A., Bryk, V.V., Vasilenko, R.L., Voevodin, V.N., Ovcharenko, V.D., Tolmacheva, G.N., Kolodii, I.V., Lunev, V.M., and Klimenko, I.O., *Vopr. At. Nauki Tekh.,* 2015, no. 2 (96), p. 111.
20. Johanson, S.A., Campbell, J.L., and Malquist, K.G., *Principles Particle Induced X-Ray Emission Spectrometry (PIXE),* New York: Wiley, 1995.
21. *Diagrammy sostoyaniya dvoinykh metallicheskikh system. Spravochnik* (State Diagrams of Binary Metal Systems. Handbook), Lyakishev, N.P., Ed., Moscow: Mashinostroenie, 1997, vol. 2.
22. Hofsas, H., *Forward Recoil Spectrometry,* New York: Plenum, 1996.
23. Egorov, V.K., Egorov, E.V., and Afanas'ev, M.S., *Bull. Rus. Acad. Sci.: Phys.,* 2014, vol. 78, no. 6, p. 498.

Translated by N. Goryacheva